

## Article

# Mycosynthesis, Characterization of Zinc Oxide Nanoparticles, and Its Assessment in Various Biological Activities

Asif Kamal <sup>1</sup>, Malka Saba <sup>1,\*</sup>, Khetab Ullah <sup>1</sup>, Saeedah Musaed Almutairi <sup>2</sup>, Bandar M. AlMunqedhi <sup>2</sup> and Mohamed Ragab abdelGawwad <sup>3</sup> 

<sup>1</sup> Department of Plant Sciences, Faculty of Biological Sciences, Quaid-i-Azam University, Islamabad 45320, Pakistan

<sup>2</sup> Department of Botany and Microbiology, College of Science, King Saud University, P.O. 2455, Riyadh 11451, Saudi Arabia

<sup>3</sup> Genetics and Bioengineering, Faculty of Engineering and Natural Sciences, International University of Sarajevo, 71210 Sarajevo, Bosnia and Herzegovina

\* Correspondence: msaba@qau.edu.pk

**Abstract:** In recent years, nanotechnology has become one of the emerging fields of nanoparticle synthesis using biological processes. The use of mushroom extract is one of the most important methods for biological synthesis due to the presence of abundant biologically active compounds. In this study, Zinc Oxide nanoparticles (ZnO NPs) were synthesized using *Daedalea* sp. mushroom extract. The nanoparticles had an average size of 14.58 nm and irregular morphology, which shows its prominent character. Various analytical techniques including FTIR, X-ray diffraction, EDX, and UV-Vis spectrum showed a broad absorption between 350 and 380 nm, which indicates the synthesis of ZnO NPs. The characterized NPs were exploited for a wide range of biomedical applications including biocompatibility, antifungal, antileishmanial, and antibacterial studies. The ZnO nanoparticles showed a strong antibacterial effect against gram-positive (*Klesbsilla pneumonia* and *Staphylococcus aureus*) and gram-negative (*Eschericia coli* and *Pseudomonas aeruginosa*) bacteria. Furthermore, the ZnO nanoparticles also showed a high antifungal effect against *Aspergillus niger* fungus.

**Keywords:** mushroom; nanoparticles; zinc oxide; biological application; *Aspergillus niger*



**Citation:** Kamal, A.; Saba, M.; Ullah, K.; Almutairi, S.M.; AlMunqedhi, B.M.; Ragab abdelGawwad, M. Mycosynthesis, Characterization of Zinc Oxide Nanoparticles, and Its Assessment in Various Biological Activities. *Crystals* **2023**, *13*, 171. <https://doi.org/10.3390/cryst13020171>

Academic Editors: Abdur Rauf and Mujeeb Ur Rehman

Received: 25 November 2022

Revised: 1 January 2023

Accepted: 2 January 2023

Published: 18 January 2023



**Copyright:** © 2023 by the authors. Licensee MDPI, Basel, Switzerland. This article is an open access article distributed under the terms and conditions of the Creative Commons Attribution (CC BY) license (<https://creativecommons.org/licenses/by/4.0/>).

## 1. Introduction

Nanoscience and nanotechnology are rising as new emerging and fast-growing fields of science with diverse areas of applications in the manufacturing of various materials at the level of the nanoscale Albrecht, 200 [1]. Because of their phenomenal properties and unique characteristics, nanoparticles (NPs) recently gained importance in various fields of science, i.e., energy sectors, healthcare fields, agriculture, environmental sciences, etc. [2]. Nanotechnology is mostly concerned with the preparation of nanoparticles of variable shape, size, chemical composition, and controlled dispersity as well as their potential use for human benefit. Nanoscience deals with the synthesis of small particles termed NPs. Nanotechnology is the study of biological activities at a nanosized scale at which their size is less than 100 nm [3]. The pattern of biological science and nanotechnology has created a new pathway for research activity in numerous biological fields. Bio-assisted or green nanoparticle synthesis methods make use of natural resources or biological systems to create metallic nanoparticles. Plant extracts, bacteria, viruses, fungi, actinomycetes, and yeasts are just a few of the natural sources used in nanoparticle green production.

To overcome biological challenges, nanobiotechnology allows us to create new smart materials from modified biological components. ZnO nanoparticles are environment-friendly, nontoxic, biocompatible, and easy to produce, making them ideal candidates for biological applications [4]. A zinc oxide nanoparticle is mainly concentrated because of its wide band gap and huge excitation energy when used in different devices such as solar cells,

batteries, photodetectors, nanolasers varistors, and biosensors. Zinc is widely recognised as an essential trace element that can be found in all bodily tissues, including the brain, muscle, bone, and skin. Zinc participates in the body's metabolism and performs critical roles in protein and nucleic acid synthesis, hematopoiesis, and neurogenesis, acting as a key component of many enzyme systems [5]. Because of the small particle size of nano-ZnO, zinc is more easily absorbed by the body. As a result, nano-ZnO is frequently utilised in food. Furthermore, the US Food and Drug Administration has classified ZnO as a "GRAS" (generally regarded as safe) chemical (FDA). ZnO NPs, which are relatively affordable and less toxic than other metal oxide NPs, have a wide range of medicinal uses, including anticancer, drug delivery, antimicrobial, diabetic treatment, anti-inflammation, wound healing, and bioimaging [6]. The toxicity of ZnO NPs and other metal oxide nanoparticles to mammalian cells and organs has been studied, and ZnO NPs have been found to cause more severe damage than other metal oxide nanoparticles in several circumstances. For example, [7] found that when neuro2A (mouse neuroblastoma, CCL131, ATCC) was exposed to ZnO nanoparticles at concentrations of 100 g/mL or higher, the cells became abnormally large and shrank. The ZnO nanoparticles reduced mitochondrial activity significantly at concentrations of 50 to 100 g/mL. In cells exposed to ZnO nanoparticles, lactate dehydrogenase leakage and apoptosis were also found [8].

The studies [9,10] used *protabello* mushroom extract for the synthesis of gold nanoparticles, and their characterization based on SEM indicated spherical, hexagonal, and triangular structures. An XRD study also identified a crystalline structure in the mycosynthesized nanoparticles, and FTIR showed a broad peak at  $3358\text{ cm}^{-1}$ , indicating an (OH) group in sugar. The characterization and antimicrobial activity of ZnO nanoparticles from *Xylaria acuta* have been compared against gram-positive and gram-negative bacteria, and their antifungal activity has been compared against plant pathogens. These myogenic ZnO nanoparticles are hexagonal in shape and size ranging from 34 to 55 nm. They show significant activity against anti-cancer at 1  $\mu\text{m}$  concentration.

Myconanotechnology is a new science for the synthesis of nanoparticles that uses fungi such as *Fusarium oxysporum*, *Colletotrichum* sp., *Trichothecium* sp., *Trichoderma asperellum* [11], *T. viride* [12], *Phanerochaete chrysosporium* [13], *F. solani* [14], *F. semitectum* [15], *A. fumigatus* [16], *Coriolus versicolor* [17], *Aspergillus niger* [18], *Phoma glomerata*, and *Penicillium brevicompactum* [19]. The fungus species were chosen for their tolerance and ability to bioaccumulate metals [20]. Mycomaterials include distilled materials such as enzymes/proteins, polysaccharides, and protein complexes, or crude extracts such as fruiting body extracts, fungal mycelia extracts, and free cell filtrate. In this study, we firstly used *Daedalea* sp. mushroom to synthesize ZnO nanoparticles to describe their characterization and antimicrobial activity. The SEM results indicated a spherical shape, the XRD results indicated a crystalline nature, and the EDX results indicated the relative percentage of zinc and oxygen. The mycosynthesized ZnO NPs showed good results against the pathogenic fungus *Aspergillus* and MTT. These nanoparticles are non-homolactic for human RBCs. Overall, our results also show that *Daedalea* Mushroom can be used to synthesize ZnO NPs. These nanoparticles are spherical in structure and nontoxic in nature for humans. The ZnO nanoparticles have a large surface area to volume ratio so they can strongly bind to the cell surface of a fungus, directly enter the cell, and damage the cell wall of the fungus, due to their small size [21].

## 2. Materials and Methods

In the present study, zinc oxide NPs were synthesized using mycosynthesis and green procedures. The precure salt used for the synthesis of zinc nanoparticles was zinc acetate dehydrated Zn  $(\text{CH}_3\text{COO})_2 \cdot 2\text{H}_2\text{O}$  with a purity of 99% (Sigma-Aldrich MERCK, Karachi, Pakistan). The mushroom extract was used as a reducing agent for the green and mycosynthesis of zinc oxide nanoparticles.

### 2.1. Collection of Mushroom Material

The mushroom sample was collected from QAU, Islamabad Pakistan in August 2020, and the sample was identified using a morphological tool.

### 2.2. Morphological Identification

The collected fungus was identified up to the generic level as *Daedalea* sp. using available morphological keys for polypores [22].

### 2.3. Mycosynthesis of ZnO NPs from *Daedalea* sp.

For the synthesis of zinc oxide nanoparticles, 10 g of the mushroom sample was added to 100 mL of distilled water and then 100 mL of an aqueous mushroom extract was slowly mixed into 100 mL of a zinc solution. For the preparation of the zinc solution, an appropriate molar mass of zinc acetate dihydrate (183.48 g/mol multiplied by 1000 = 0.183 × 100 = 18.348 × 0.1 = 1.834 gm of zinc salt) was added into 100 mL of distilled water to prepare the salt solution of zinc oxide nanoparticles. These salt solutions were added to 100 mL of the mushroom extract. These solutions were kept on a hot plate for 6 h at a temperature of 100 °C with a magnetic stirrer set at 250 rpm. The colour of the zinc oxide solution remained. The pH of zinc oxide was 1.9. Centrifugation was completed at 15,000 rpm for 15 min. After centrifugation, the supernatant was discarded. After washing, the nanoparticles were transferred into a petri dish and dried on a hot plate at 300 °C. The dry particles were ground into a fine powder and stored at room temperature for further chemical and physical characterization.

### 2.4. Characterization of Zinc Oxide Nanoparticles from *Daedalea* sp.

#### 2.4.1. UV-Vis Spectrophotometry Analysis

The optical properties of the mycosynthesized ZnO NPs were determined using a Perkin-Elmer lambda spectrophotometer. The reflectance spectra of the prepared samples were obtained at room temperature at a range of wavelengths between 360 and 380 nm.

#### 2.4.2. XRD Analysis

The crystalline structure of the ZnO NPs was confirmed using X-ray Diffraction (XRD) analysis in the 2θ range of 10°–70°. The analysis used a PAN analytical Emprean Diffractometer with Cu Kα radiation ( $\lambda = 1.5406\text{\AA}$ ) and Bragg-Brentano  $\theta$ – $\theta$  configuration.

#### 2.4.3. SEM and EDX

The morphology and elemental composition of the mycosynthesized ZnO NPs were determined using a scanning electron microscope (SEM, NovaSEM450 operated at 20 Kv) with energy dispersive X-ray (EDX) spectroscopy (IT100LA).

#### 2.4.4. FTIR Analysis

Different chemical bonds present in the biosynthesized ZnO NPs were identified using Fourier-transform infra-red (FTIR) analysis within the 400–4000  $\text{cm}^{-1}$  range.

### 2.5. Biological Application

#### 2.5.1. Antifungal Activity of Zinc Oxide NPs

A comparison of the antifungal activity of the mycosynthesized iron and zinc nanoparticles against *aspergillus* was performed using the well-diffusion method. Different concentrations of zinc and iron 24 nanoparticles (0.25, 0.50, 0.75 mL) were made to check the antifungal activity. Each concentration was added to PDA media separately, and three replicates of each concentration were made. The isolated fungus was excised into about 2–4 mm inoculum discs and placed in the centre of the PDA media plates accurately in sterilized conditions. Different concentrations of nanoparticle treatments were administered to the fungus on separate PDA media plates, and the plates without nanoparticle treatment served as the positive control. These PDA media plates were kept in an incubator for one

week at  $26 \pm 27$  °C, after which the fungi showed different growth inhibition at different concentrations of nanoparticles. In all Petri plates, the growth inhibition was estimated using the following formula:

$$\text{Growth inhibition\%} = (C - T) / C \times 100$$

### 2.5.2. Antibacterial Activity

The antibacterial activity of the ZnO NPs was tested against four strains of bacteria using the disc diffusion method. The bacteria included two gram-positive bacterial strains (*Klesbsilla pneumonia* and *Staphylococcus aureus*) and two gram-negative bacterial strains (*Eschericia coli* and *Pseudomonas aeruginosa*). In this method, 4 mg/mL of the ZnO NPs sample was prepared in 1 ml of DMSO. Then, a sterile paper disk impregnated with a solution of the compounds was kept on the surface of the agar plates that were inoculated with the pathogen bacteria. These plates were incubated for 24 h at 37 °C, after which the size of the inhibitory zones around the discs was measured.

### 2.5.3. Biocompatibility

The hemolytic activity assay of the RBCs–NPs interaction was conducted to evaluate the toxic nature of mycosynthesized ZnO NPs using freshly obtained human blood. A total of 1 cc of blood was collected from volunteers having no other health issues. To prevent coagulation, blood was collected in an EDTA tube (Khalil et al., 2017). The blood was centrifuged at 15,000 rpm for 5 min to obtain fresh RBCs and separate plasma. RBCs were obtained in a pellet after repeating the centrifugation 2–3 times. Later, 9.8 mL of PBS (phosphate buffer saline) was added to 200 µL of freshly obtained pellet erythrocytes. Then, mixing was completed using proper shaking of the solution in PBS. The NP samples at four different concentrations, 20 µL, 40 µL, 60 µL, and 80 µL, were added to the suspended erythrocytes in a 1.5 mL Eppendorf tube. The mixture was then incubated at 35 °C for 1 h. Then, centrifugation of the incubated sample was carried out at 10,000 rpm for 10 min. The supernatant was obtained, of which 100 µL was poured into 96 well plates. The absorbance of the obtained supernatant was measured at 541 nm using a spectrophotometer. Triton X-10 was used as a positive control and DMSO as a negative control. The calculation of the percent hemolytic activity of RBCs by NPs was evaluated using the following percentage formula:

$$\% \text{ Hemolysis} = \{(\text{sample abs} - \text{neg. control abs}) / (\text{positive control abs} - \text{negative control abs})\} \times 100$$

### 2.5.4. Anti-Leishmanial Activity

*Leishmania tropica*, a well-known leishmanial parasite, was tested against the samples for leishmnaicidal activity (KWH23). Both the promastigote (flagellar) and amastigote (aflagellate) forms were subjected to the assay. Both the promastigotes and the amastigotes were freshly cultivated and kept overnight in an appropriate medium (MI99 with 10% FBS) for the experiment. At the time of the assay, 20 L of the test sample and 180 L of the refreshed culture were gently mixed in a separate 96-well plate. The plates were then incubated for 3 days at room temperature (25 °C), followed by a further 72 h of incubation at the same temperature. Amphotericin-B was used in the experiment as a positive control (PC), while DMSO was used as a negative control (NC). Following the initial incubation period, each well of the plate was filled with 20 L of MTT solution (4 mg/mL DW) and set aside at room temperature for a second incubation. At 540 nm, the plate's absorbance was measured, and the following equation was used to calculate the percentage of inhibition:

$$\% \text{ Inhibition} = \left[ 1 - \left\{ \frac{\text{Absample}}{\text{Abcontrol}} \right\} \right] \times 100.$$

### 3. Results and Discussion

#### 3.1. XRD Study

The XRD study determined the crystallinity of the synthesized nanoparticles. The XRD spectrum of the mycosynthesized zinc oxide nanoparticles identified the structural properties. The crystals are regular arrays of atoms. The phase identification, purity, and crystallite size confirmed using the XRD patterns are shown in Figure 1. The ZnO NPs have a hexagonal crystalline structure and presented distinct diffraction in the spectra that were analogues to peak values of (100), (002), (101), (102), (110), (103), (200), (112), (201) and (202), respectively [23]. The acquired result is in good agreement with the standard JCPDS card no. 01-1136. The average crystalline size of the zinc oxide nanoparticles was 14.53 nm as determined from the XRD spectra using Debye Scherer's formula:

$$D = k \cdot \lambda / \beta \cos \theta \quad (1)$$

where D is average crystallite size, k is Debye Scherer's constant ( $k = 0.94$ ),  $\lambda$  is the wavelength of incident Cu  $\alpha$  radiation (0.154 nm),  $\beta$  is FWHM of the peak, and  $\theta$  is the Bragg's angle.

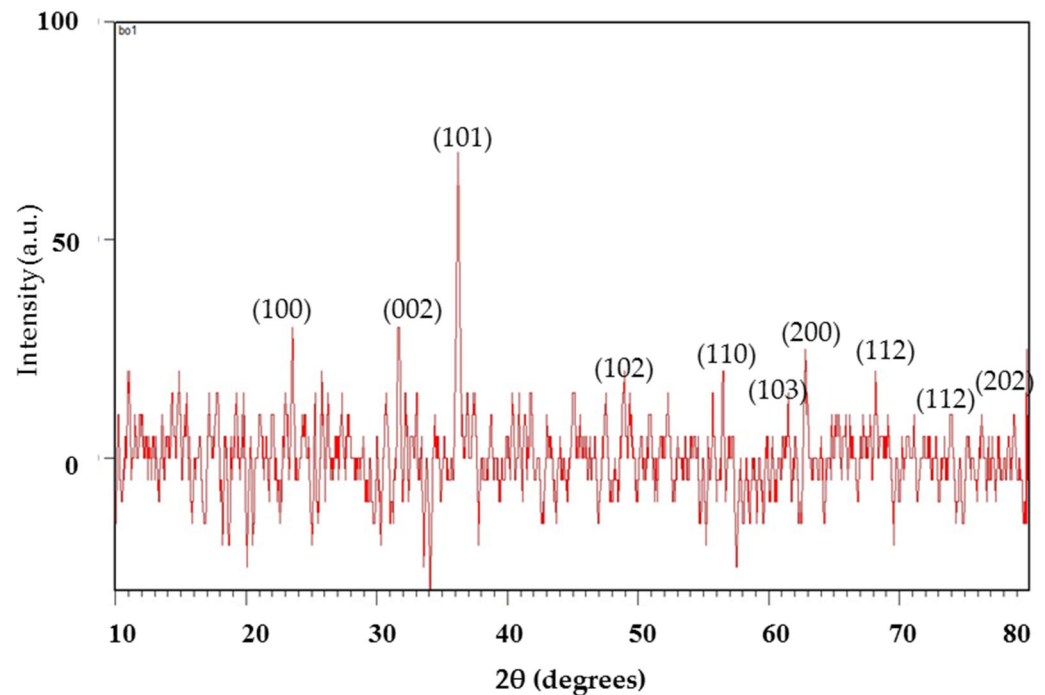
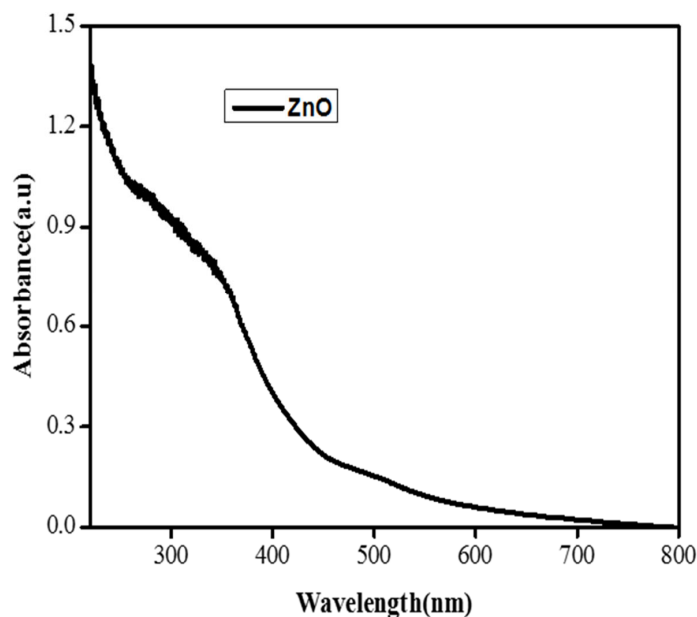


Figure 1. X-ray diffraction pattern of the ZnO nanoparticles.

#### 3.2. UV Analysis

The synthesis of the ZnO NPs was determined using spectral analysis with a UV-Vis spectrophotometer. The UV/Visible study was carried out to obtain information about the band gap of iron nanoparticles using the following method. The UV/Visible study was also carried out to obtain information about the optical properties of the synthesized iron oxide nanoparticles. The UV spectra were analyzed in a range of 200–800 nm. The ZnO nanoparticles mainly show absorption peaks at wavelengths of 370 nm, which indicate the formation of zinc oxide NPs. The UV visible spectra of zinc oxide nanoparticles showed various peaks in the range between 350 and 380 nm as shown in Figure 2 [24].



**Figure 2.** UV pattern of the ZnO nanoparticles.

### 3.3. FTIR Study

The FTIR study was performed to determine the functional groups present in the mycosynthesized zinc oxide nanoparticles. The measurements were recorded in the spectral range of  $400\text{ cm}^{-1}$  to  $4000\text{ cm}^{-1}$ , which showed various absorption bands. The mycosynthesized zinc oxide nanoparticles showed the phenolic OH group present in the IR spectrum and confirmed the possible mechanism for the formation of zinc oxide nanoparticles. The FTIR analysis showed various peaks which indicate that the characteristic functional groups exist in the synthesized zinc oxide NPs. The peak at  $3266.22\text{ cm}^{-1}$  describes the strong O–H band of the alcohol. The absorption peaks at  $1549.76\text{ cm}^{-1}$  and  $1407\text{ cm}^{-1}$  represent the vibrational modes of the N–O strong bond of the nitro compound and the C–H medium band of the alkane compound, respectively. The peaks at  $669.07\text{ cm}^{-1}$  are ascribed to the C–Br strong halo compound [25]. The complete spectra is shown in Figure 3.

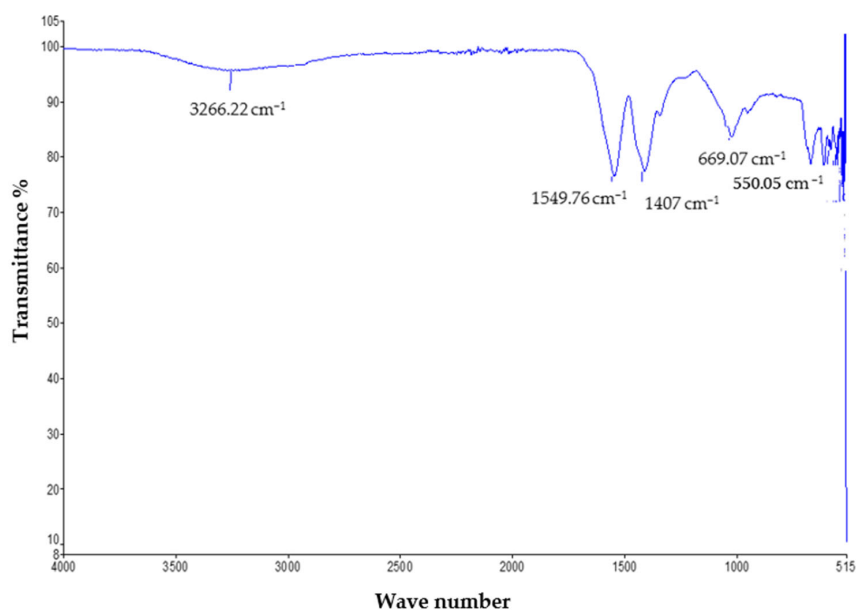


**Figure 3.** FTIR analysis of the ZnO nanoparticles.

### 3.4. EDX Analysis

The existence of the element zinc oxide can be identified using EDX analysis, which indicates the reduction of a zinc ion into a zinc element in the reaction mixture. The elemental composition analysis of zinc nanoparticles revealed the presence of Zn and O in the sample and confirmed the high purity of the synthesized zinc oxide nanoparticles. The relative percentage of zinc and oxygen in the mycosynthesized zinc nanoparticles (58.34% of zinc and 13.28% oxygen) individually are similar to theoretical expectations based on the stoichiometric mass present, and the percentage of other elements are shown in Figure 4 and Table 1 [26].

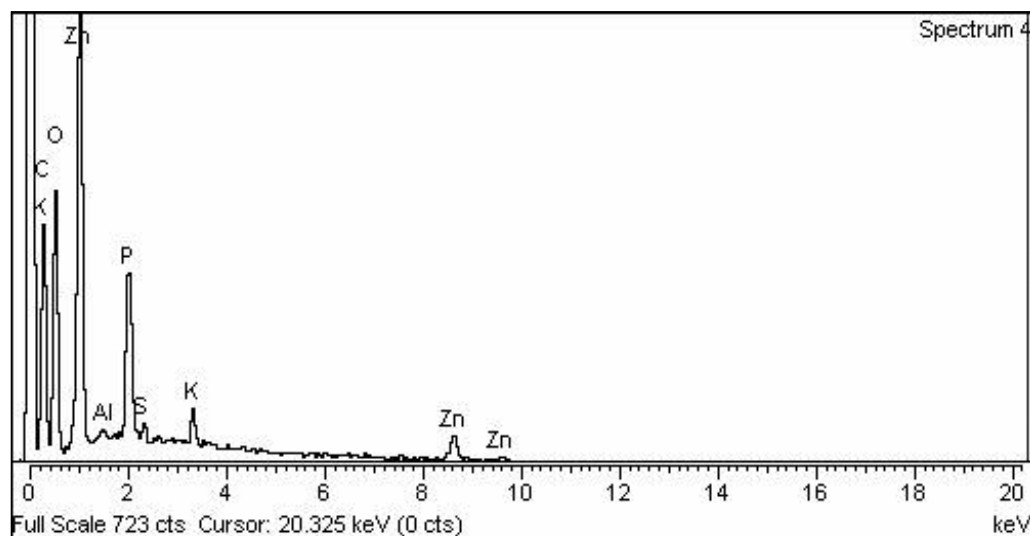


**Figure 4.** EDX spectrum of the zinc oxide nanoparticles.

**Table 1.** Elemental composition of ZnO nanoparticles after EDX analysis.

Element	Weight%	Atomic%
C k	24.30	52.68
O K	13.28	21.62
P K	18	1.51
Cu K	2.28	0.94
Zn k	58.34	23.24

### 3.5. SEM Study

The SEM micrograph of the synthesized zinc oxide nanoparticles was used to study the surface morphology of the particles. The nanoparticles were agglomerated and aggerated, as can be seen in the SEM image, due to the presence of sticky wild mushroom extract over the surface of the ZnO NPs, which acts as a capping and stabilizing agent (Figure 5). The agglomeration can be removed using the addition of surfactant, but this will lead to a loss of the potential characteristics of nanoparticles. In our study, the SEM images obtained of the mycosynthesized zinc oxide nanoparticles were nearly irregular in shape, which is aligned with the results of previously published literature [27].

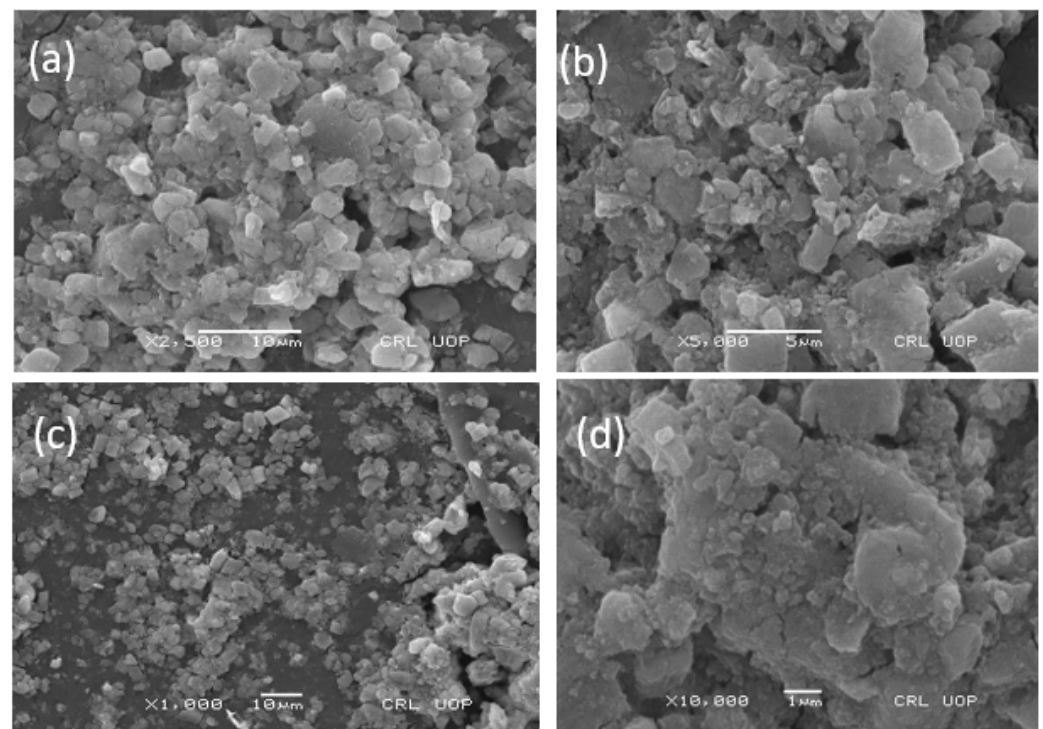


**Figure 5.** (a) 2500 resolution (b) 5000 resolution and (c,d) are same resolution of Scanning electron microscopy image of the zinc oxide nanoparticles at various magnifications.

### 3.6. Biological Application

#### 3.6.1. Antifungal Activity

The antifungal assay was conducted according to the procedure that was adopted for zinc oxide. Briefly, a pathogenic fungus, *Aspergillus niger*, was collected from the Molecular Plant Pathology laboratory, department of plant science Quaid-i-Azam university Islamabad, and the antifungal assay was performed using the agar well diffusion method with some variation. The autoclaved PDA media with zinc oxide nanoparticles at different concentrations of NPs (1 mg/mL, 0.75 mg/mL, 0.5 mg/mL, 0.25 mg/mL, 0.1 mg/mL) solution was poured into the Petri dishes. After the PDA media solidified, the fungus was injected. The ability of zinc oxide nanoparticle treatment was estimated at time intervals of 6 days using measurements of the diameter of fungal growth. All tests were performed in triplicate, and the values were expressed in cm. The growth of the fungus was measured at different concentrations of zinc oxide nanoparticles (Figure 6). At 0.25 mg/mL concentration, the fungus growth was 88%. At 0.5 mg/mL concentration, the growth inhibition of the fungus was 70%. At 0.75 mg/mL concentration, the fungus growth inhibition was 75%. This result showed that the higher nanoparticle concentration of 0.75 mg has a high growth inhibition of 75%. The lower concentration (0.25 mg/mL) has minimum growth inhibition 88% as shown in Table 2 [28].

**Table 2.** Antifungal activity of the zinc oxide nanoparticles.

Concentration	Control	% Inhibition
0.1 mg	9 cm	22%
0.25 mg	9 cm	88%
0.5 mg	9 cm	70%
0.75 mg	9 cm	75%
1.0 mg	9 cm	68%

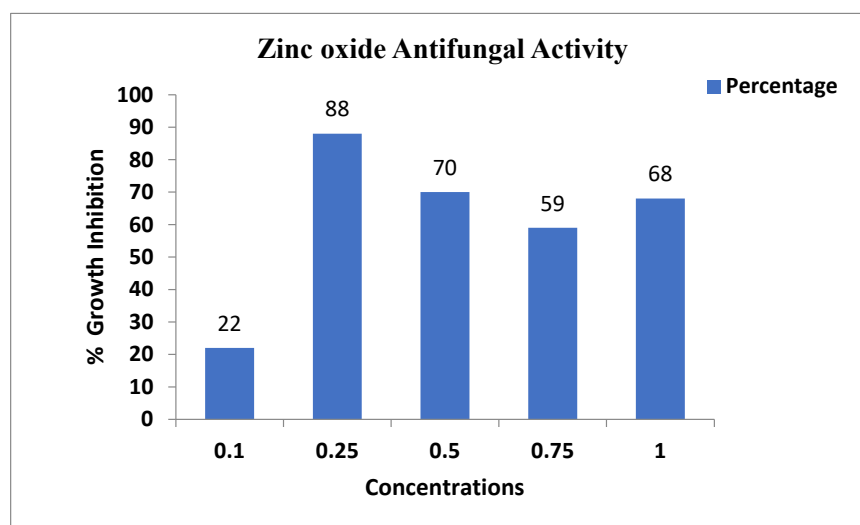


**Figure 6.** Antifungal activity of the zinc oxide nanoparticles against *Aspergillus*.

### 3.6.2. Antibacterial Activity

The antibacterial activity of the mycosynthesized ZnO NPs made using the mushroom extract of *Daedalea* was tested against four strains of bacteria, i.e., *S. aureus*, *P. aureginosa*, *E. coli*, and *Klesbsilla pneumonia*. The mycosynthesized ZnO NPs showed a positive result against all strains of bacteria. The bactericidal effect of the mycosynthesized ZnO NPs was found to be higher against gram-negative than against gram-positive bacteria due to the structural differences between them. The mycosynthesized ZnO NPs synthesized from *Daedalea* sp. revealed an efficient zone of inhibition for *P. aureginosa* (7 mm), *E. coli* (10 mm), *S. aureus* (7 mm), and *K. pneumonia* (7 mm) as shown in Table 2. Similar results were reported in the literature [29]. The antibacterial activity of ZnO NPs was found to be higher when compared to others due to the disruptive effect of NPs on microbial membranes by radical formation, i.e., oxides or hydroxyl radicals, which destroy bacterial membranes. In addition, the high surface area of NPs enables them to enter bacteria via pores in the plasma membranes by proteins. Furthermore, the high surface area enhances more contact or friction with bacterial cells, which causes more compounds and extracts to enter the cells of microbes. Finally, the release of  $H_2O_2$  from the surface of the ZnO NPs was reported as destructive against microbes. The formation and release of  $H_2O_2$  are dependent on which surface the ZnO NPs are found.  $H_2O_2$  penetrates the cells of microorganisms resulting in death [30]. The whole antibacterial is shown in the Figure 7 and Table 3.

**Table 3.** Antibacterial Activity of The Mycosynthesized Zinc Oxide Nanoparticles.

Pathogenic Bacteria	ZnO NPs 4 mg/mL	Positive Control
<i>E. coli</i>	10 ± 0.34	20 ± 0.39
<i>P. aeuroginose</i>	7 ± 0.40	15 ± 0.35
<i>S. aeururs</i>	7 ± 0.35	8 ± 0.37
<i>K. pneumonia</i>	7 ± 0.42	20 ± 0.34

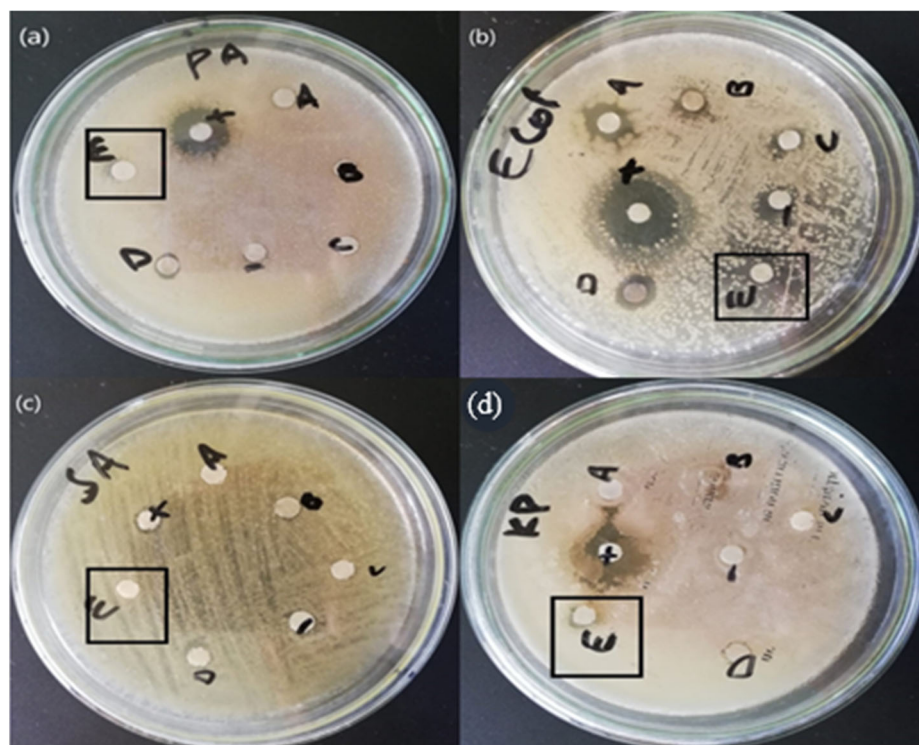


**Figure 7.** (a) *P. aeruginosa* (b) *E. coli* (c) *S. aureus* (d) *K. pneumonia* Antibacterial activity of the zinc oxide nanoparticles.

### 3.6.3. Biocompatibility

To evaluate the safe nature and the toxicity of NPs, their interaction with human blood was carried out using biosynthesized ZnO NPs. Based on the results, it is clear that NPs are nontoxic to normal cells. The hemolytic activity of NPs was determined and compared to the values according to the standard of the “American society for testing and materials designation”. Based on these standards, any type of NPs or other material having  $\geq 5\%$  hemolysis is considered hemolytic, others having 2–5% are mild hemolytic, and others having  $\leq 2\%$  are considered safe and non-hemolytic [30]. The hemolysis activity of NPs was measured upon the rupturing of RBCs and release of hemoglobin to the medium when treated with the NPs (4 mg/mL). The results show that the ZnO NPs are mildly hemolytic and can be used for various biological applications. These findings and results are comparable with previous studies [31]. The percentage hemolysis is shown in the Table 4.

**Table 4.** Percent Hemolysis of the ZnO NPs.

S. No	Conc mg/mL	% Hemolysis
1	400	0.048 ± 2
2	200	0.064 ± 4
3	100	0.047 ± 6
4	50	0.047 ± 8
Control		0.210

### 3.6.4. Antileishmanial Activity

In the antileishmanial activity analysis, the mycosynthesized ZnO NPs were evaluated against Leishmaniasis, an infectious disease primarily brought on by the parasite *Leishmania*. While the infection has been endemic in 100 countries, leishmaniasis has an annual incidence rate of 1.5 to 2 million worldwide. Sand flies carry the intracellular leishmania

parasite to people's bodies. Phlebotomus and Lutzomyia, which bite, spread the illness. This disease is highly likely to be spread uncontrollably due to inappropriate vectors. The cytotoxic effects of the formulations of mycosynthetically synthesized Zn ONPs were tested between 50 and 400 g/mL on both amastigote and *L. tropica* promastigote cultures. As can be seen, cytotoxicity at different doses was found to be effective against the promastigote and amastigote forms of the parasite, with favourable mortality rates of 77% 1.4 and 74% 1.6 at 400 g/mL. Additionally, significant LC 50 values of 220 g/mL for promastigote (Phlebotomus and Lutzomyia) bites and 270 g/mL for amastigote were reported for both patristic forms [32]. The Antileishmanial Activity is shown in the Table 5.

**Table 5.** Percent mortality of amastigote and promastigote parasites, in vitro cholinesterase potential of the ZnO NPs.

Con (ug/m)	Promastigote Inhibition	Amastigote	IC50 (ug/mL)	IC50 (ug/mL)
400	60.21	54.78	270 Amas	220 Prom
200	49.33	44.0		
100	37.33	31.45		
50	23.10	18.19		

#### 4. Conclusions

The wild mushroom *Daedalea* sp. can be used for the synthesis of zinc oxide nanoparticles. The aqueous extract of the wild mushroom containing carbohydrates, proteins, and phenolic compounds was responsible for the formation of the stabilizing and capping agent of particles. The FTIR analysis confirmed the functional group present in the zinc oxide nanoparticles at the peak range of  $3266.22\text{ cm}^{-1}$ . The sharper and stronger diffraction peak observed in the XRD analysis confirmed the crystallinity of the mycosynthesized zinc oxide nanoparticles. Mycosynthesize zinc oxide nanoparticles have a size range of 14.53 nm and were found to be irregular in shape, as confirmed using SEM analysis. The different functional groups of zinc oxide NPs, including O–H, N–O, C–H, and C–Br, make the synthesized zinc oxide nanoparticles an effective antimicrobial agent. Synthesized zinc oxide nanoparticles can be used for their effective antifungal activity.

**Author Contributions:** Conceptualization, A.K. and M.S.; methodology, A.K., M.S. and M.R.a.; software, A.K., K.U. and M.S.; validation, A.K., K.U. and M.S.; formal analysis, A.K. and S.M.A.; investigation and resources, M.S.; data curation, K.U. and A.K.; writing—original draft preparation, A.K., B.M.A. and M.R.a.; writing—review and editing, S.M.A. and B.M.A.; visualization, S.M.A. and A.K.; supervision and project administration, M.S. All authors have read and agreed to the published version of the manuscript.

**Funding:** The authors extend their appreciation to the Researchers Supporting Project number (RSP2023R470), King Saud University, Riyadh, Saudi Arabia.

**Conflicts of Interest:** The authors declare that they have no conflict of interest.

#### References

- Albrecht, M.A.; Evans, C.W.; Raston, C.L. Green chemistry and the health implications of nanoparticles. *Green Chem.* **2006**, *8*, 417–432. [CrossRef]
- Aula, M.; Leppänen, A.; Roininen, J.; Heikkinen, E.-P.; Vallo, K.; Fabritius, T.; Huttula, M. Characterization of process conditions in industrial stainless steelmaking electric arc furnace using optical emission spectrum measurements. *Metall. Mater. Trans.* **2014**, *45*, 839–849. [CrossRef]
- Balashanmugam, P.; Santhosh, S.; Giyaullah, H.; Balakumaran, M.; Kalaichelvan, P. Mycosynthesis, characterization and antibacterial activity of silver nanoparticles from *Microporus xanthopus*: A macro mushroom. *Int. J. Innov. Res. Sci. Eng. Technol.* **2013**, *2*, 6262–6270.
- Brindhadevi, K.; Samuel, M.S.; Verma, T.N.; Vasantharaj, S.; Sathiyavimal, S.; Saravanan, M.; Duc, P.A. Zinc oxide nanoparticles (ZnONPs)-induced antioxidants and photocatalytic degradation activity from hybrid grape pulp extract (HGPE). *Agric. Biotechnol.* **2020**, *28*, 101730. [CrossRef]

5. Chin, S.F.; Azman, A.; Pang, S.C. Size controlled synthesis of starch nanoparticles by a microemulsion method. *J. Nanomater.* **2014**, *22*, 3388. [[CrossRef](#)]
6. Dheyab, M.A.; Owaied, M.N.; Rabeea, M.A.; Aziz, A.A.; Jameel, M.S. Mycosynthesis of gold nanoparticles by the Portabello mushroom extract, Agaricaceae, and their efficacy for decolorization of Azo dye. *Environ. Nanotechnol. Monit. Manag.* **2020**, *14*, 100312. [[CrossRef](#)]
7. Faisal, S.; Khan, M.A.; Jan, H.; Shah, S.A.; Shah, S.; Rizwan, M.; Akbar, M.T. Edible mushroom (*Flammulina velutipes*) as biosource for silver nanoparticles: From synthesis to diverse biomedical and environmental applications. *Nanotechnology* **2020**, *32*, 065101. [[CrossRef](#)] [[PubMed](#)]
8. He, L.; Liu, Y.; Mustapha, A.; Lin, M. Antifungal activity of zinc oxide nanoparticles against *Botrytis cinerea* and *Penicillium expansum*. *Microbiol. Res.* **2011**, *166*, 207–215. [[CrossRef](#)]
9. Mohamed, Y.; Azzam, A.; Amin, B.; Safwat, N. Mycosynthesis of iron nanoparticles by *Alternaria alternata* and its antibacterial activity. *Afr. J. Biotechnol.* **2015**, *14*, 1234–1241. [[CrossRef](#)]
10. Naeem, G.A.; Jaloot, A.S.; Owaied, M.N.; Muslim, R.F. Green synthesis of gold nanoparticles from *Coprinus comatus*, agaricaceae, and the effect of ultraviolet irradiation on their characteristics. *WJST* **2021**, *18*, 9396. [[CrossRef](#)]
11. Hengstmengel, J. Notes on *Hymenoscyphus* 3: On the nomenclature of *Hymenoscyphus subcarneus* (Ascomycota, Helotiales). *Mycotaxon* **2009**, *107*, 267–276. [[CrossRef](#)]
12. Rajabi, H.R.; Naghiha, R.; Kheirizadeh, M.; Sadatfaraji, H.; Mirzaei, A.; Alvand, Z.M. Microwave assisted extraction as an efficient approach for biosynthesis of zinc oxide nanoparticles: Synthesis, characterization, and biological properties. *Mater. Sci. Eng. C* **2017**, *78*, 1109–1118. [[CrossRef](#)] [[PubMed](#)]
13. Geiser, D.M.; Aoki, T.; Bacon, C.W.; Baker, S.E.; Bhattacharyya, M.K.; Brandt, M.E.; Zhang, N. One fungus, one name: Defining the genus *Fusarium* in a scientifically robust way that preserves longstanding use. *Phytopathology* **2013**, *103*, 400–408. [[CrossRef](#)] [[PubMed](#)]
14. Santa Izabel, T.S.; Cruz, A.C.R.; Gusmão, L.F.P. Conidial fungi from the semi-arid Caatinga biome of Brazil. *Ellisembiopsis* gen. nov., new variety of *Sporidesmiella* and some notes on *Sporidesmium* complex. *Mycosphere* **2013**, *4*, 156–163. [[CrossRef](#)]
15. Ahmed, K.; Valeem, E.E.; Khan, M.A. Biosynthesis of alpha amylase from *Aspergillus Fumigatus* (Fresenius 1863) in submerged fermentation. *PJBT* **2015**, *12*, 87–92.
16. Zhao, K.; Wu, G.; Feng, B.; Yang, Z.L. Molecular phylogeny of *Caloboletus* (Boletaceae) and a new species in East Asia. *Mycol. Prog.* **2014**, *13*, 1127–1136. [[CrossRef](#)]
17. Burdsall, H.H., Jr.; Larsen, M.J. *Lazulinospora*, a new genus of Corticiaceae, and a note on *Tomentella atrocyanea*. *Mycologia* **1974**, *66*, 96–100. [[CrossRef](#)]
18. Vinokurova, N.G.; Baskunov, B.P.; Zelenkova, N.F.; Arinbasarov, M.U. The alkaloids of *Penicillium aurantiogriseum* Dierckx (1901) var. *aurantiogriseum* VKM F-1298. *Microbiology* **2004**, *73*, 414–419. [[CrossRef](#)]
19. Thompson, F.; Gomez-Gil, B. International Committee on Systematics of Prokaryotes Subcommittee on the taxonomy of Aeromonadaceae, Vibrionaceae and related organisms Minutes of the meeting, 13 November 2017, Chicago, USA. *Int. J. Syst. Evol. Microbiol.* **2018**, *68*, 2111–2112. [[CrossRef](#)]
20. Sharmila, G.; Muthukumaran, C.; Sandiya, K.; Santhiya, S.; Pradeep, R.S.; Kumar, N.M.; Thirumarimurugan, M. Biosynthesis, characterization, and antibacterial activity of zinc oxide nanoparticles derived from *Bauhinia tomentosa* leaf extract. *J. Nanostruct. Chem.* **2018**, *8*, 293–299. [[CrossRef](#)]
21. Sumanth, B.; Lakshmeesha, T.R.; Ansari, M.A.; Alzohairy, M.A.; Udayashankar, A.C.; Shobha, B.; Almatroudi, A. Mycogenic synthesis of extracellular zinc oxide nanoparticles from *Xylaria acuta* and its nanoantibiotic potential. *Int. J. Nanomed.* **2020**, *15*, 8519. [[CrossRef](#)]
22. Vithiya, K.; Sen, S. Biosynthesis of nanoparticles. *Int. J. Pharm. Sci.* **2011**, *2*, 2781.
23. Rani, V.; Verma, Y.; Rana, K.; Rana, S.V.S. Zinc oxide nanoparticles inhibit dimethylnitrosamine induced liver injury in rat. *Chem. Biol. Interact.* **2018**, *295*, 84–92. [[CrossRef](#)]
24. Huang, X.; Zheng, X.; Xu, Z.; Yi, C. ZnO-based nanocarriers for drug delivery application: From passive to smart strategies. *Int. J. Pharm.* **2017**, *534*, 190–194. [[CrossRef](#)]
25. Jeng, H.A.; Swanson, J. Toxicity of metal oxide nanoparticles in mammalian cells. *J. Environ. Sci. Health A* **2006**, *41*, 2699–2711. [[CrossRef](#)]
26. Wojnarowicz, J.; Chudoba, T.; Lojkowski, W. A review of microwave synthesis of zinc oxide nanomaterials: Reactants, process parameters and morphologies. *Nanomaterials* **2020**, *10*, 1086. [[CrossRef](#)]
27. Zubair, M.S.; Munis, M.F.H.; Alsudays, I.M.; Alamer, K.H.; Haroon, U.; Kamal, A.; Ali, M.; Ahmed, J.; Ahmad, Z.; Attia, H. First Report of Fruit Rot of Cherry and Its Control Using Fe<sub>2</sub>O<sub>3</sub> Nanoparticles Synthesized in *Calotropis procera*. *Molecules* **2022**, *27*, 4461. [[CrossRef](#)]
28. Bavarsad, M.; Farrokhi-Nejad, R. Identification of *Trichoderma* Species Using Partial Sequencing of nrRNA and tef1 $\alpha$  Genes with Report of *Trichoderma capillare* in Iran Mycoflora. *Majallah-I Hifāzat-I Giyāhān* **2018**, *113*, 5874.
29. Bocci, F.; Gearhart-Serna, L.; Boareto, M.; Ribeiro, M.; Ben-Jacob, E.; Devi, G.R.; Jolly, M.K. Toward understanding cancer stem cell heterogeneity in the tumor microenvironment. *Proc. Natl. Acad. Sci. USA* **2019**, *116*, 148–157. [[CrossRef](#)]
30. Han, M.L.; Vlasak, J.; Cui, B.K. *Daedalea americana* sp. nov. (Polyporales, Basidiomycota) evidenced by morphological characters and phylogenetic analysis. *Phytotaxa* **2015**, *204*, 277–286. [[CrossRef](#)]

31. Rajabi, M.; Mousa, S.A. The role of angiogenesis in cancer treat. *Biomedicines* **2017**, *5*, 34. [[CrossRef](#)]
32. Rabeea, M.A.; Owaid, M.N.; Aziz, A.A.; Jameel, M.S.; Dheyab, M.A. Mycosynthesis of gold nanoparticles using the extract of *Flammulina velutipes*, Physalacriaceae, and their efficacy for decolorization of methylene blue. *J. Environ. Chem. Eng.* **2020**, *8*, 103841. [[CrossRef](#)]

**Disclaimer/Publisher's Note:** The statements, opinions and data contained in all publications are solely those of the individual author(s) and contributor(s) and not of MDPI and/or the editor(s). MDPI and/or the editor(s) disclaim responsibility for any injury to people or property resulting from any ideas, methods, instructions or products referred to in the content.